OPERATIONAL RELIABILITY AND ACCURACY OF SODARS IN WING VORTEX CHARACTERIZATION

Stuart G Bradley[*]
University of Auckland, Auckland, New Zealand

Sabine von Hünerbein
University of Salford, Manchester, UK

Ken Underwood
Atmospheric Systems Inc., Los Angeles, California

1. INTRODUCTION

The lift maintaining aircraft in flight comes from a bound circulation around the aircraft wings. At the wing tips this circulation becomes a pair of trailing vortices, with a strong combined downwash between them. The vortices are relatively long-lived because of their angular momentum, and interact with each other and the prevailing atmospheric conditions (particularly wind shear and temperature inversions), making their longevity, strength, and location difficult to predict. Since a sudden unpredicted downwash is a hazard to following aircraft at the critical times of landing or taking off, considerable effort has been expended by many workers in attempting to provide real-time remote sensing measurement tools.

Amongst the remote sensing technologies, LIDAR provides quite good real-time capture of vortex properties, but does suffer from problems in the presence of precipitation or fog, or indeed very clean air. Acoustic radars, known as SODARs, obtain strong reflections of acoustic pulses from atmospheric turbulence, and the Doppler shift allows wind vector components to be measured, generally about every 10-15 m up to a height of 200-500m. In contrast to LIDARs, SODARs measure through fog and in clean air and at least operate in precipitation (but with mixed effectiveness). This means that an all-weather system for characterizing vortices might best comprise an integration of LIDAR and SODAR technologies.

Bradley et al. (2006) show that high-quality real-time measurements of wing vortex strength and position can be obtained using well-established SODAR technology. Their method uses individual SODAR profiles of vertical wind from four SODARs placed in a line perpendicular to, and on one side of, the flight path near the end of the runway. Bradley (2006) examines optimal numbers of SODARs. In either case, though, this is an unusual and demanding use of SODAR technology since no signal averaging is used to obtain these 'snap-shots' of the vertical wind structure.

The back-scattered acoustic power is extremely weak, so SODARs generally average 50 or more power spectra at each height range in order to obtain good estimates of the Doppler-shifted frequency at the spectral peak. In order to track development and position of individual vortices it is however necessary to obtain wind profiles every few seconds. For an initial vortex height of 100 m, the return time for a sound pulse is about 0.6 s, so only about 4 profiles can be averaged. Bradley et al. (2006) describe a SODAR array in which pulses were transmitted every 2 s and individual profiles were analyzed. The decrease in signal-to-noise ratio (SNR) is however compensated to some degree by doing a non-linear least-squares fit of the instantaneous vertical velocity field to a simple vortex model. This inherently emphasizes signal in comparison to noise, providing that the model adequately describes the underlying physical situation.

The purpose of this paper is to investigate the likely limitations in use of SODARs to characterize vortex strength and position, given the need to average over a very small number of profiles. We include the main influences which are known to cause signal loss, and give an overview of their likely contribution in the context of a major airport.

2. DATA AVAILABILITY IN SODARS

Here we review and evaluate those situations known to cause reduced data availability. SODARs receive energy back-scattered from turbulent fluctuations. This is described by the SODAR equation

$$P_R \;=\; P_T G A_e \frac{cT}{2}\left[\frac{e^{-2\alpha z}}{z^2}\right]\sigma_s + P_N \qquad (1)$$

where P_R is the *received* power which depends on the transmitted power P_T, the antenna transmitting efficiency G, the antenna effective receiving area A_e, the pulse duration T, the height z, the absorption coefficient of air α, the speed of sound c, and the scattering cross section σ_s per unit solid angle per unit volume of air. The first few terms in (1) are primarily determined by system design. The term in square brackets represents transmission losses, and $\sigma_s = \sigma_T + \sigma_R + \sigma_C$ depends on the scattering cross sections of turbulence (σ_T), rainfall (σ_R) and ground clutter 'fixed echoes' (σ_C). The dependence on transmitted frequency f_T is $\alpha \propto f_T^2$ (for absorption in air), $\sigma_T \propto f_T^{1/3}$, and $\sigma_R \propto f_T^4$. Reflections from surrounding objects, included through σ_C, are to first order independent of f_T. Background noise power contributes through P_N. The Doppler shift, which gives the wind information, is contained in the σ_T term, so it is important that all of the following hold.

(a) $\quad \dfrac{P_N}{P_R} \ll 1 \qquad$ low background noise

(b) $\quad \dfrac{\sigma_R}{\sigma_T} \ll 1 \qquad$ low rainfall scatter

(c) $\quad \dfrac{\sigma_C}{\sigma_T} \ll 1 \qquad$ low fixed echo.

We will discuss each of these conditions below.

2.1 Definition of data availability

Because the loss factor becomes increasingly dominant at greater heights, one or more of the conditions (a), (b), and (c) above eventually fail during a profile. Detection of this failure is subjective, but a common method is to compare the integrated signal power around the highest (or most likely) spectral peak with the power in the wings of the spectrum or from a spectrum at great height (both of these should give noise power). In the discussions below we assume that failure of signal peak detection occurs when noise power equals the 'signal' power (i.e. SNR = 0 dB).

2.2 Low-turbulence (σ_T too small)

Either low turbulence (usually a result of low wind shear) and/or negligible vertical temperature gradient (a neutral temperature profile), will result in little vertical turbulent transport of warmer air patches into colder air, or in other words low acoustic refractive index variability. This situation leads to low σ_T and a reduced range under which the SODAR gets valid data. Field results from Bradley et al. (2005) from a small Scintec SODAR are shown in Fig. 1.
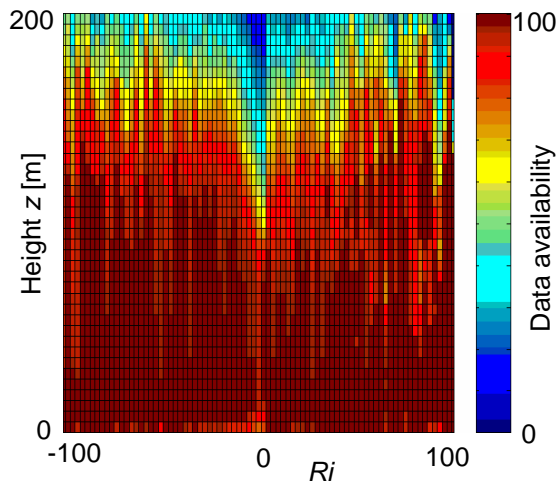

Figure 1. Percentage of relative data yield of SODAR receptions, plotted against height z and against the Richardson number Ri based upon meteorological mast measurements at 100 m.

However, for the case of aircraft vortices, the vortex-associated wind shear is very large and local turbulence is readily generated by this. Furthermore, airports have a large concrete surface component which tends to emphasize thermal contrasts and lead to either nocturnal stable temperature profiles or daytime unstable profiles. The wing vortices are a *forced* mixing of air at different heights (rather than buoyancy-driven mixing), which enhances any thermal contrasts and leads to much higher acoustic backscatter. Consequently, the vortex situation is one in which SODARs can be expected to perform particularly well because of high σ_T.

2.3 Rainfall ($\sigma_R \geq \sigma_T$)

Based on acoustic Rayleigh scattering from the widely used exponential distribution of raindrop sizes (see for example, Bradley and Webb, 2002), rain has a scattering cross-section given by

$$\Delta \sigma_R = \frac{\pi^5 f_T^4}{36 c^4} N_D D^6 e^{-\Lambda D} \Delta D \qquad (2)$$

for raindrops having diameters between D and $D+\Delta D$. The constants are $N_D = 8 \times 10^6$ m^{-4} and $\Lambda = 4100\, R^{-0.21}$ m^{-1}, for rainfall intensity R measured in mm h^{-1}. For a vertical SODAR beam, drops in this diameter range contribute echo power in the Doppler frequency interval f_D to $f_D+\Delta f_D$ where

$$f_D = f_T \left(1 + \frac{2}{c} 4874 D e^{-195 D} \right) \qquad (3)$$

is calculated from a simple formula for drop terminal fall speed V_T. Fig. 2 shows actual measurements using a 4500 Hz SODAR. The central peak is due to turbulent scatter from air having almost no vertical motion and the peaks to the right are due to falling raindrops.

For a SODAR having T = 33 ms, the spectral width of the echo signal from turbulence is about 2/T = 60 Hz. Typically σ_T =10^{-11} m^{-1} sr^{-1}, c = 340 m s^{-1} and f_T = 4 kHz. Using (2) and (3), these numbers allow the SNR, given by σ_T divided by the corresponding $\Delta \sigma_R$, to be calculated as a function of vertical wind speed w and rainfall intensity R. Results are shown in Fig. 3.
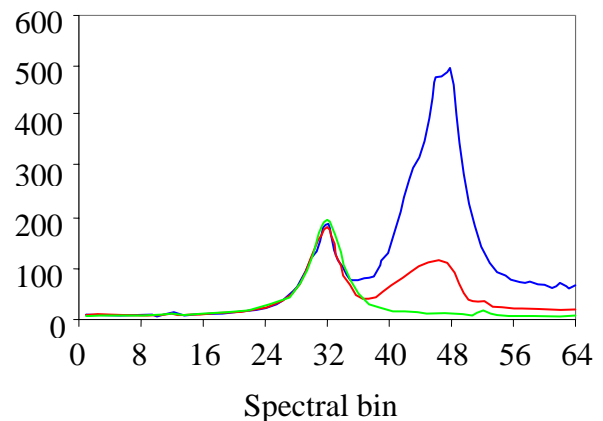

Figure 2. Spectra from a 4500 Hz SODAR for no rain (green), 5-10 mm h^{-1} (red), and >10 mm h^{-1} (blue).
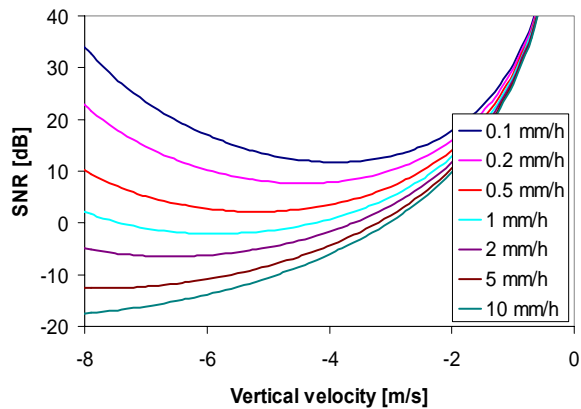
Figure 3. SNR for different vertical velocities of the air and for different rainfall intensities.

It can be seen that, consistent with the measurements shown in Fig. 2, problems really only occur for rainfall rates above about $R = 1$ mm h^{-1}. For strong downdrafts, only the larger drops have comparable fall speeds, and their numbers are small: this causes the increase in SNR with increasing downdraft, except for the heaviest rain.

These results are obtained assuming that the raindrops are falling at their terminal speed with respect to the ground, and that they have not changed their speed to that of the local air. Clearly this assumption is not valid for the smaller drops and even the largest drops may respond significantly to the local air velocity in a vortex. In order to evaluate this effect, we write the *upward* acceleration of an individual drop in the form

$$a = \frac{F_{drag}}{m} - g \qquad (4)$$

where F_{drag} is the drag force on the drop due to air flow over it, and g is the acceleration due to gravity. To first order, F_{drag} equals pressure times drop cross section area so, for the case of a drop accelerating into still air, (4) can be rewritten in the form

$$\frac{dV}{dt} = k\frac{V^2}{D} - g . \qquad (5)$$

Since $a=0$ when terminal speed is reached, $k = gDV_T^{-2}$. Integration shows that the response time constant is approximately $\tau = 2V_T/(3g)$.
For a single vortex at the origin, the vertical velocity is given by

$$w = \frac{\Gamma}{2\pi}\frac{x}{x^2 + z^2} \qquad (6)$$

and $\Gamma \approx 300$ m^2 s^{-1} for a large jet.

The drop velocity profiles in Fig. 4 indicate that all drops follow the vortex vertical velocities to a large extent. This means that the broad Doppler spectrum from the rain will largely shift with the local wind speed. But there are differences between the shapes of the profiles on the updraft and downdraft sides of the vortex, and also phase lags for large drops due to their inertia.
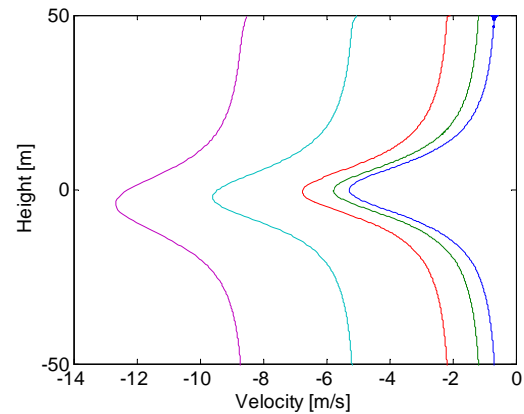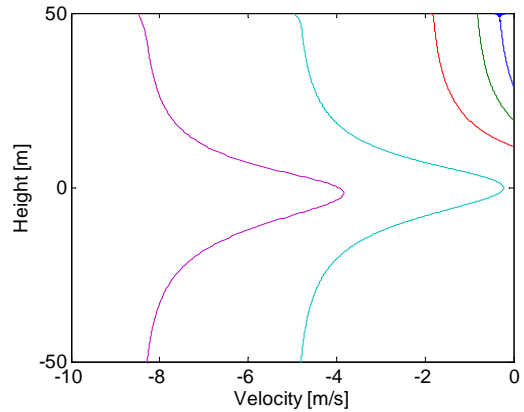

Figure 4. Velocity-height profiles for drops falling 1 m either side of the core of a vortex with $\Gamma=300$ m^2 s^{-1}. Drops are falling at terminal speed 50 m above the core.

The conclusion is that it is important to distinguish the turbulence reflection for the rain reflection in order to obtain good quality wind estimates, but that reasonable estimates of vortex core position and strength may be available even in heavy rain by analyzing the differential variations in the Doppler spectrum. This latter idea warrants further investigation because in heavy rain there is still a strong echo signal available from the rain.

2.4 High background noise levels ($P_N \geq P_R$)

The SNR, for the narrow frequency band of interest, is generally quite low, and typically in the range 0-20 dB.
However, this in-band acoustic background noise is not appreciably worse in airport environments. For example, Fujii et al. (2001) have analysed acoustic noise from a landing jumbo jet at Nagoya Airport and made data and analysing software available at http://www.ymec.com/hp/signal2/air1.htm.
Fig. 5 shows a spectrogram of relative intensities from an aircraft landing. The spectrum is relatively flat in the band from 1 kHz to 6 kHz generally used by SODARs. These data were scaled to the equivalent of 118 dB intensity level, typical of that from a 747-400 at 60 m height. Corrections were then made to allow for the frequency bin size in the spectrum. Finally, a typical spectrum from a

turbulence echo was added. This was based on $P_R = 10^{-13}$ W, $A_e = 0.2$ m^2, and $\tau = 33$ ms. The result in Fig. 6 shows that a typical echo signal is perhaps 10 dB above the aircraft noise signal. This agrees with actual experience operating at airports.
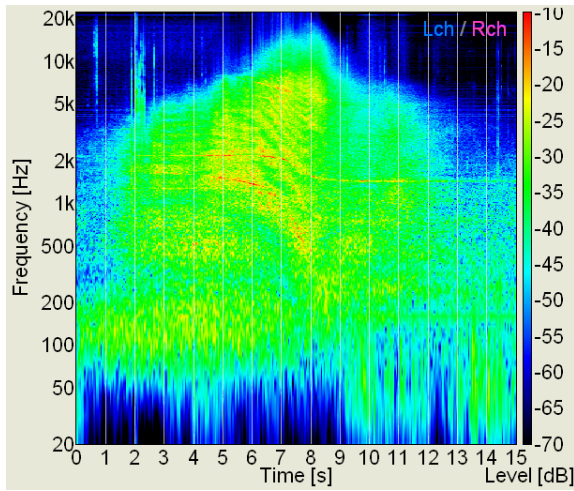

Figure 5. A spectrogram of acoustic noise from a landing jet aircraft.

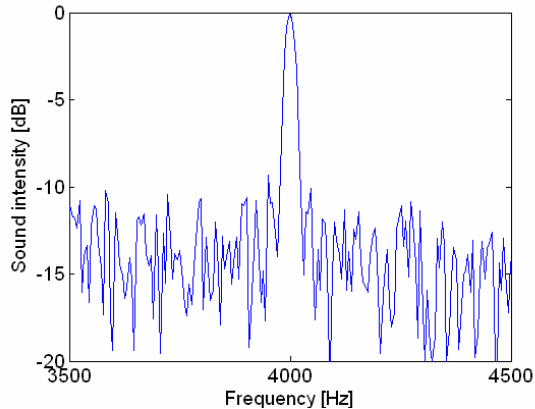Note that other background acoustic noise will generally make the SNR lower than shown in Fig. 6.

Figure 6. Spectrum of SODAR signal superimposed on measured spectrum of acoustic noise due to a landing aircraft.

3. VORTEX PARAMETER ESTIMATION

Bradley et al. (2006) have analyzed SODAR measurements of vortices from landing aircraft at Vienna International. These measurements were conducted with four small (about 0.5 m high) SODARs in a line perpendicular to, and on one side of, the flight path. The SODARs were spaced by 25 m and operated about 80 m below the landing aircraft. Single profiles were obtained synchronously every 2 s and were analyzed by fitting the vertical velocity data to a simple vortex model *independently* for each profile. Results showed smoothly varying vortex strength and position.

The position and spacing of each vortex pair at each 2 s interval were determined to about 5 m, an uncertainty which is adequate for air traffic purposes. The uncertainty in vortex strength was around 25%, again acceptable for air traffic safety. Fig. 7 shows one example of estimated vortex position parameters.

Conventionally SODARs are not operated in this single-profile mode because of low SNR. In the method developed by Bradley et al. (2006), however, the low SNR is compensated by enhanced signal recovery through the least-squares fitting procedure. Only four SODARs were used in unison in this analysis: an array containing more SODARs would give even better quality estimates of vortex position and strength.
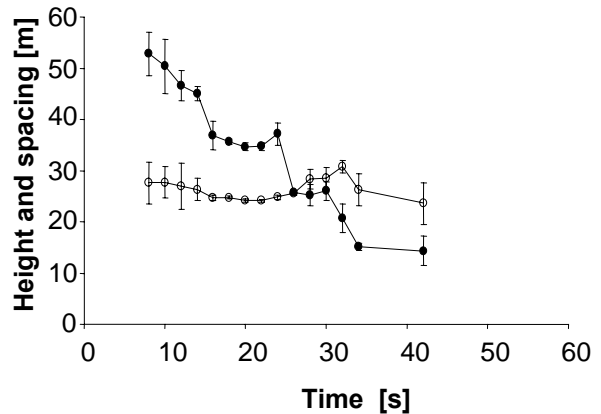

Figure 7. An example of the evolution of vortex height (filled circles) and half-spacing (open circles).

4. VORTEX PARAMETER AVAILABILITY

The data used by Bradley et al. (2006) for their analysis was obtained only from a short period of observation. For potential use as an operational tool, or even as a useful research instrument, it is important that such a SODAR array obtain data consistently.
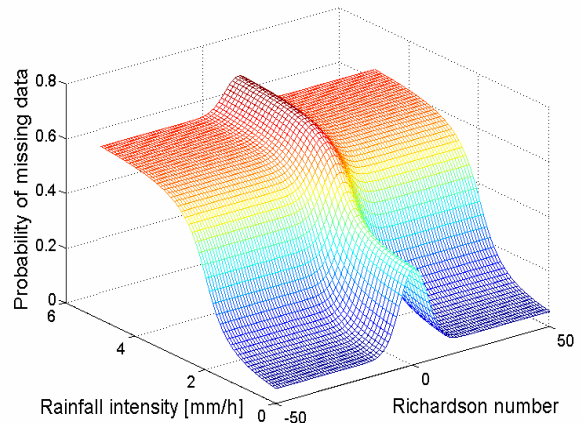

Figure 8. The probability of missing data from 100 m height, as a function of Richardson number Ri and rainfall intensity R.

From the analyses in Sections 2 and 3 above, we can make some estimates of data availability. Fig. 8 shows this in concept, but the levels need to be verified through further field testing.

This figure is simply based on the measurements and calculations for rainfall above, and on the measurements by Bradley et al. (2005) of data availability in differing atmospheric conditions on a flat site. Because of the vigorous mixing provided by the mechanical forcing from vortices, the Ri number dependence is not expected to be as strong for the vortex situation.

The probability of missing data during rain is based on the range of vertical velocities which will occur in a vortex flow. For low updrafts and downdrafts the detection of turbulent motion should be possible in even quite heavy rain. Similarly, for strong updrafts and downdrafts the turbulent motion will be detectable in moderate rain because there are not many drops having comparable fall speeds and contributing in that part of the Doppler spectrum. So the drop-outs in data will be from moderate updrafts and downdrafts in moderate-to-heavy showers.

Given the ensemble least-squares approach taken by Bradley et al. (2006), drop-outs of data from the mid-range of air velocities will only partly compromise retrieval of vortex position and strength. This topic is considered in more detail by Bradley (2006).

5. SUMMARY

We have evaluated the common causes of data loss in SODARs: low back-scatter; rainfall; and high background acoustic noise. Contrary to intuition, high background acoustic noise is not expected to be particularly problematic at airports. This finding is supported by measurement experience at many airports.

Low back-scatter, due to low thermal or refractive index contrast, has been found to be a major cause of data loss in other field experiments, particularly at elevated heights. However, the vortex situation is rather different in three aspects:

- most interest is in heights from 0-100 m
- airports are high thermal contrast sites
- vortices provide mechanical mixing

These factors are expected to strongly increase data availability.

Acoustic back-scatter from rainfall is expected to be the main cause of data loss. However, our analysis suggests:

- data loss is negligible for $R < 1$ mm h^{-1}
- data loss in heavy rain is only partial

This means that a scheme such as that of Bradley et al. (2006) should be capable of retrieving valid vortex position and strength information even during moderate-to-heavy rainfall.

These findings are based on actual SODAR measurements involving vortex parameter estimation, operation in neutral atmospheres, and operation during rain, but *not* for combinations of these situations. Therefore more definitive work is required based on field measurements over an extended time at airfields.

6. REFERENCES

Bradley S.G. and T. Webb, 2002. Use of an ultrasonic SODAR to sense raindrop size distributions. *J. Atmos. Oceanic Technol.*, **19**, 1203-1207.

Bradley, S. G. (ed), Antoniou, I., S. von Hünerbein, Kindler, D., de Noord, M., and H. E. Jorgensen, 2004. *SODAR calibration for wind energy applications.* Final reporting on WP3 EU WISE project NNE5-2001-297. 69pp.

Bradley, S. G., E. Mursch–Radlgruber, E. and S. von Hünerbein, 2006. SODAR Measurements of Wing Vortex Strength and Position. Submitted to *J. Ocean. Atmos. Tech..*

Bradley, S. G., 2006. Validation of SODAR real-time sensing and visualisation of wake vortices. *Paper P5.10, 12th Conf. Aviation Range and Aerospace Met., AMS, Atlanta.*

Fujii, K., Y. Soeta, and Y. Ando, 2001. Acoustical properties of aircraft noise measured by temporal and spatial factors. *J. Sound and Vibration*, **241**, 69-78.